Penerbit Akademia Baru

CFD Letters

Journal homepage: www.akademiabaru.com/cfdl.html
ISSN: 2180-1363

Numerical Investigation of Flow Field of a Non-Circular Cylinder

Open Access

Muhammad Fahmi Mohd Sajali[1], Abdul Aabid[1], Sher Afghan Khan[1,*], Fharukh Ahmed Ghasi Mehaboobali[2,3], Erwin Sulaeman[1]

[1] Department of Mechanical Engineering, Faculty of Engineering, International Islamic University Malaysia, 53100, Kuala Lumpur, Malaysia
[2] Department of Mechanical Engineering, Bearys Institute of Technology, Mangalore, Karnataka, India
[3] Department of Mechanical Engineering, Government Engineering College, Huvinahadagali, Karnataka, India

ARTICLE INFO

Article history:
Received 27 February 2019
Received in revised form 24 April 2019
Accepted 18 May 2019
Available online 20 May 2019

Keywords:
ANSYS, CFD, D-shaped model, Pressure drag, and Flowfield.

ABSTRACT

The study of the base flow field or the flow field in the wake region is not accessible by using only a theoretical method; mostly this study has been done experimentally. The problem statement of this study is to know the effect of flow past of a non-circular cylinder on the drag. At high Reynolds number, the flow past a bluff body is characterized by a large wake zone. Therefore, drag reduction of the flow field is an interesting problem with a wide range of application. The present paper presents the numerical simulation of the flow field of a non-circular cylinder. The shielding effect of the square-plate front body on the flow field of drag reduction and the pressure distribution of a three-dimensional bluff body is simulated by using a numerical method. The results obtained from the simulation are compared with the experimental results. The results indicate that the side faces and the rear faces are subjected to low pressure, whereas the front face is experiencing high positive pressure. With this flow pattern, the pressure drag coefficient assumes a substantially significant value in the range of 1.0 - 1.42. Such a high value of drag coefficient is particularly valid for bluff bodies with noncircular cross-sections with sharp corners.

1. Introduction

The study of the base flow field is a prevalent practical problem with a wide range of applications. At high enough Reynolds numbers, the flow past a bluff body is characterized by a large wake zone. The separated shear layers from the sharp corners feed vorticity to the wake. These vorticities are shed continuously downstream. The front body drag is like a resistance that reduces the speed of the vehicle and increases its vibration and finally resulting in decreased range and lower efficiency. It is essential to reduce the front body drag in order to produce high speed, to reduce vibration, to enhance the range, and fuel efficiency. Given the depleting fossil fuel scenario, aerodynamic shape optimization becomes essential for sustainable development. This front body effect on the drag and flow field of a noncircular cylinder is related to the aerodynamics of the shape as well as the type of

* *Corresponding author.*
E-mail address: sakhan06@gmail.com (Sher Afghan Khan)

flow whether the flow is laminar or turbulent. The optimum aerodynamic shape will result in minimum front body drag and the higher fuel efficiency. The present study aims to reduce the front body drag by passive means. In this analysis, the ANSYS software is used as the primary tool to carry out the numerical investigation of drag and flow field in a non-circular cylinder. The pressure versus the body of the non-circular cylinder is computed by using ANSYS Fluent. This result will be used to do the analyses of the front body effect on the drag and the flow field of a non-circular cylinder.

Sowoud *et al.,* [1] identified the flow field, and the result can be seen from the experiment conducted. Then, the pressure coefficient, C_P is examined for with pipe and without pipe for a speed of 20.38 m/s. Once the pressure coefficient, C_P is determined, the drag coefficient C_D is evaluated for both cases: with a pipe, and without pipe. The numerical simulation of this model is not conducted earlier. Hence, in order to validate their results with simulation, this paper aims at the validation of their experimental result. Khan *et al.,* [2–4] used a convergence-divergence nozzle with sudden expansion duct to obtain effectiveness of microjet control to control the based pressure. The author used computational fluid dynamic simulation with different parameter studies such as the effect of area ratio, length to diameter ratio, and the NPR at different Mach number. Khan *et al.,* [5] identified the supersonic flow over a delta wing through an ANSYS simulation.

Suresh *et al.,* [6] determine the simulation result to compare with the experimental result. However, the author only compared their drag coefficient, C_D with the experimental results. The author does not mention about pressure coefficient, C_P. The flow field is also not shown in their studies. So, in this present study, we aim to conduct a simulation using ANSYS to simulate the pressure distribution and the pressure coefficient (C_P) and compared them with the experimental results. A body which is not a streamlined body is said to be a bluff body [7]. In order to compare the variation of pressure around a bluff body for a variety of flow conditions, it is conventional to use a dimensionless parameter which is called as the pressure coefficient C_P, that compares the pressure on the surface of the non-cylinder, P, to that at infinity, P_∞ [7]. An approximate formula was developed by making use of a semi-empirical relation for the drag of an isolated disk with a cavity wake, where C_D is the drag coefficient of the disk based on its diameter [8]. The nature of the wake is more influential than the bluff body itself [9]. Other than that, the boundary layer effects might be caused the wake around the bluff body [10].

There are three different types of flow regimes and pattern which could be identified for strakes close to the corner, optimum strakes configuration and strakes close to the center [11]. They also found that another factor that contributes towards drag reduction is the novel technique used in the generation of significant suction over the windward face [11]. Next, is the separations from bluff bodies which are of two types they are the sharp-edged, and a continuous surface where the boundary layer fails to withstand critical adverse pressure gradient [12]. The measurements on circular cylinders have shown that a curved or serrated separation line inhibited the periodic vortex shedding and thus created a steady base flow behind the cylinder, with a corresponding increase in the base pressure [13]. The CFD is a numerical simulation technology used for the solution of the governing fluid flow equations and the heat transfer inside a defined flow geometry [14]. Computational Fluid Dynamics (CFD) is an engineering tool that assists in the experimental investigation [15].

Theoretically, it is possible to obtain the front body drag by using the analytical approach. The front body drag from the experimental method is a challenging task. The reason for this is that the rear body is exposed to a perturbed flow field and that get substantially altered by the front body. Also, there is also some upstream influence of the rear body on the front-body flow field. In experiments, the model of the prototype 3D non-circular cylinder needs to be fabricated, and then, the prototype in a wind tunnel is tested for various lengths of the front body of various sizes of the

flat plate in the front to arrive at an optimum dimension of the front body that results in minimum drag. An optimum dimension will result in reducing the drag of the body. Thus, this limitation will need to be further investigated. This study primarily consists of the 2D segment. For the 2D segment, the understanding of the front body drag is studied and explored. Next, the stag will be the analysis by observing the pressure distribution from the inlet to the outlet to understand its behavior. The Bernoulli equation is used to get the dimensionless drag coefficient and pressure coefficient. Then, the dimensionless drag coefficient and pressure coefficient is converted to normalize drag and the velocity.

2. Methodology

2.1 Finite Element Method

In this study, the finite element method is used as one of the numerical methods for solving any engineering problem. The problem in this study is about fluid flow for a non-circular cylinder flow field. ANSYS software is utilized which is a versatile technique of modeling and simulation of flow fields that provide accurate results regarding the flow characteristics of an object [16].

2.1.1 Geometry and modelling

The geometry of the finite element for fluid flow based on the designed square plate front body on the drag reduction and pressure distribution of a bluff body as shown in Figure 1. The square plate front body of the bluff body is designed whose length is 108 mm, and 100 mm width of the rear body [1] is formed to investigate the flow structure on the blunt-edged delta wing further, the team called as Vortex Flow Experiment (VFE-2). The primary objective of the VFE-2 test was to validate the results of Navier-Stokes calculations and to obtain more detailed experimental data. The VFE-2 experiments were carried out for both sharp and blunt leading-edge shape delta wing [17–20].

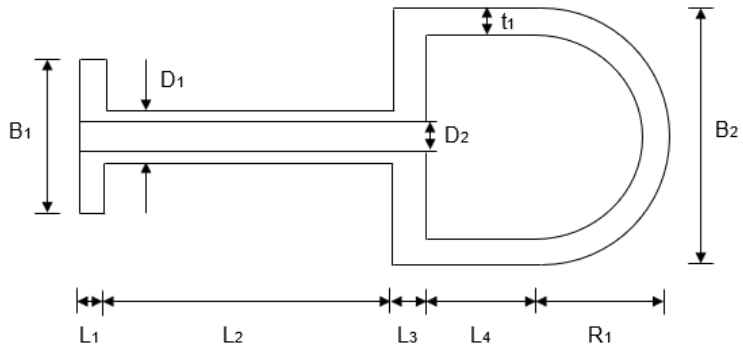

Fig. 1. Geometry of 2D Square Plate Front Body of a Bluff Body

The dimensions of the square plate bluff body are mentioned in Table 1.

Table 1
The Dimension of 2D Square Plate Front Body of a Bluff Body

B_1	B_2	D_1	D2	L_1	L_2	L_3	L_4	R_1	t_1
0.25 to 1.0B_2 (0 & 25) mm	100 mm	10 mm	8 mm	10 mm	0.25 to 2.25B_2 (0 & 100) mm	15 mm	43 mm	50 mm	8 mm

2.1.2 Two-dimensional finite element model

The two-dimensional (2D) model of a bluff body without a square plate front body is shown in Figure 2(a). The 2D model was created by using ANSYS workbench [21]. The 2D model of a square plate front body of a bluff body is shown in Figure 2(b).

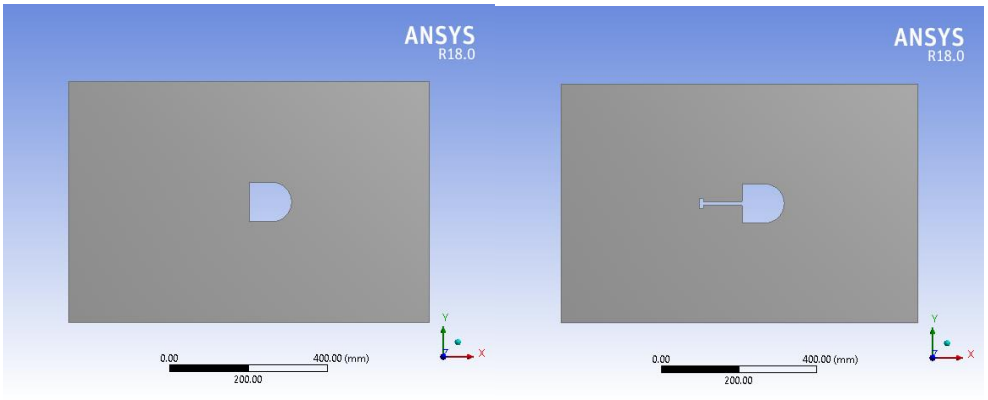

(a) (b)

Fig. 2. 2D Planar Fluid Body Finite Element (a) without Pipe (b) with Pipe

2.1.3 Meshing and boundary condition

The closed form of finite element meshing for a 2D model of a bluff body without a square plate front body is shown in Figure 3(a). Total, 20673 binary nodes were generated for the 2D planar model [3]. The closed form of finite element meshing for a 2D model of a square plate front body of a bluff body is shown in Figure 3(b). Total, 42681 binary nodes were generated for the 2D planar model [2]. The 2D model was created by using ANSYS workbench for an unstructured mesh with the number of elements has been used high to enhance fine mesh.

The meshing of the finite element for fluid flow and the number of elements used must be high to create a fine mesh in the close area at the edge of the planar body. It produces the most appropriate mesh for accurate and efficient Multi-physics solutions [2–5], [22–24]. In the present mesh, the fine mesh is used with the number of divisions for edge sizing is 100 for both cases. The mesh is high at the bluff body because we need to see the precise result for the bluff body. The volume area is not compulsory to have high mesh. The meshing is also used triangle shape for an unstructured mesh with refinement to get smooth triangle shape of mesh with a high number of the element.

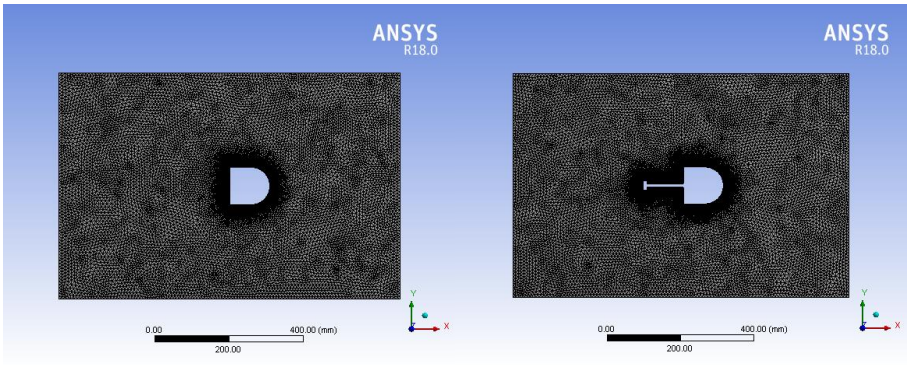

(a) (b)

Fig. 3. 2D Planar Fluid Body Meshing (a) without Pipe (b) with Pipe

2.1.4 Validation of present finite element results

In order to validate our present FE model, considered the experimental work of Sowoud *et al.,* [1]. Sowoud *et al.,* [1] have conducted experiments at the velocity of 20.38 m/s for without pipe and with pipe to see the flow field, to investigate the pressure coefficient, C_P and to determine the drag coefficient, C_D. By comparing the experimental results obtained by Sowoud *et al.,* [1] and the present simulation result, the pressure coefficient, C_P is comparable where the difference between each method is minimal and is within the acceptable limit. In this study, we are using the results without pipe and with pipe for 20.38 m/s of velocity. However, the results of the pressure coefficient, C_P for simulation is slightly different in comparison to the experimental results of the pressure coefficient, C_P. The reason for this trend may be due to the type of mesh of the model which is not a structured mesh. However, the structured mesh is more precise in term of the final outcome as compared to the unstructured mesh, but the unstructured mesh is also acceptable in some cases. They are case sensitive, and one has to deal with on a case to case basis.

The results of the pressure coefficient, C_P for simulation also is not smooth when compared with the pressure coefficient, C_P in case of the experimental data. The results obtained from simulations have some fluctuations at the mean value of the data. This is because the results obtained from the simulation have a more significant number of data point plotted such that the experimental result obtained have a limited data points which were plotted. Thus, the data point plotted for simulation results have around 1354, and 2648 data point plotted for without pipe and with pipe respectively. Whereas the experimental results have around 42 and 44 data points which were plotted for without pipe and with pipe respectively (Figure 4).

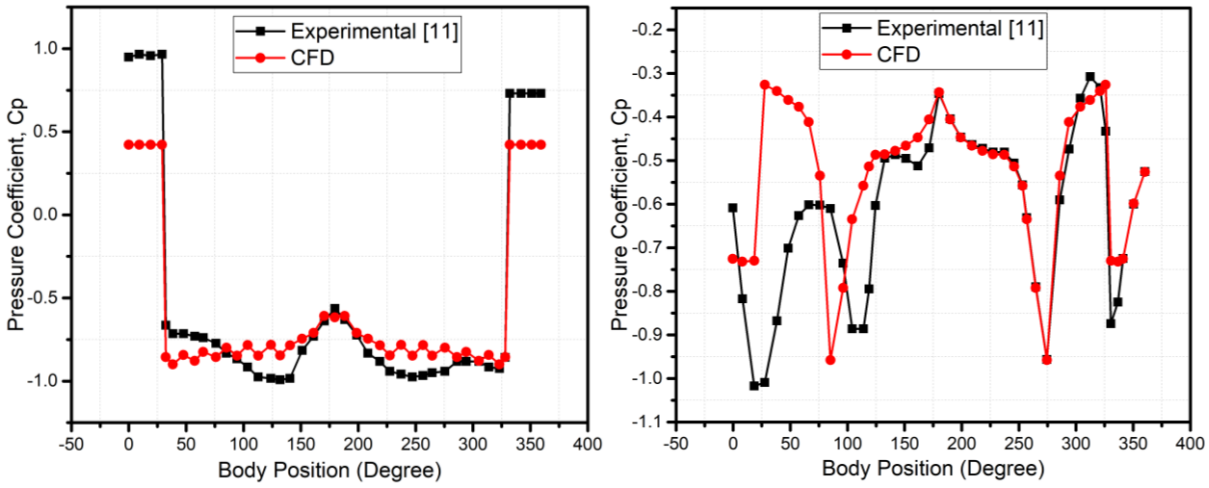

(a) (b)

Fig. 4. Validation of Result (a) without Pipe (b) with Pipe

3. Results and Discussion

The ANSYS software already has the equations that required to proceed for the computation. Hence, in this study we have used governing equations to calculate the flow parameters. The equations and the boundary conditions used in this study are as follows (Table 2 and Table 3):

Table 2
Related Equation for The study

No.	Equation's Name	Equations
1	Bernoulli's Equation	$P + \frac{1}{2}\rho V^2 + \rho gh = \text{Constant}$
2	Reynolds Number	$Re = \frac{\rho VL}{\mu}$
3	Pressure Coefficient	$C_p = \frac{P - P_\infty}{\frac{\rho V^2}{2}}$
4	Drag Coefficient	$C_D = 0.827(1 - C_p)$

Table 3
Boundary Conditions

Type	Pressure-Based
Energy Equation	On
Viscous Model	k-epsilon, Standard with Compressibility Effect
Boundary Condition	Inlet, Outlet, and Wall
Initialization Methods	Standard Initialization
Number of Iterations	10000
Reporting Interval	100
Profile Update Interval	100

3.1 Without Pipe

3.1.1 Pressure distribution

In this section we have shown the pressure variation from the inlet to the outlet of the 2D model of a bluff body without square plate front body. This pressure variation consists of dynamic pressure, static pressure, and total pressure. The numerical study was performed and verified for each case [24]. The Figure 5 to 7 show the dynamic pressure, static pressure and total pressure variation from the inlet to the outlet of the 2D model of a bluff body without square plate front body by considering contours Figure 5(a), 6(a), and 7(a) and plots respectively (Figure 5(b), 6(b), and 7(b)) respectively.

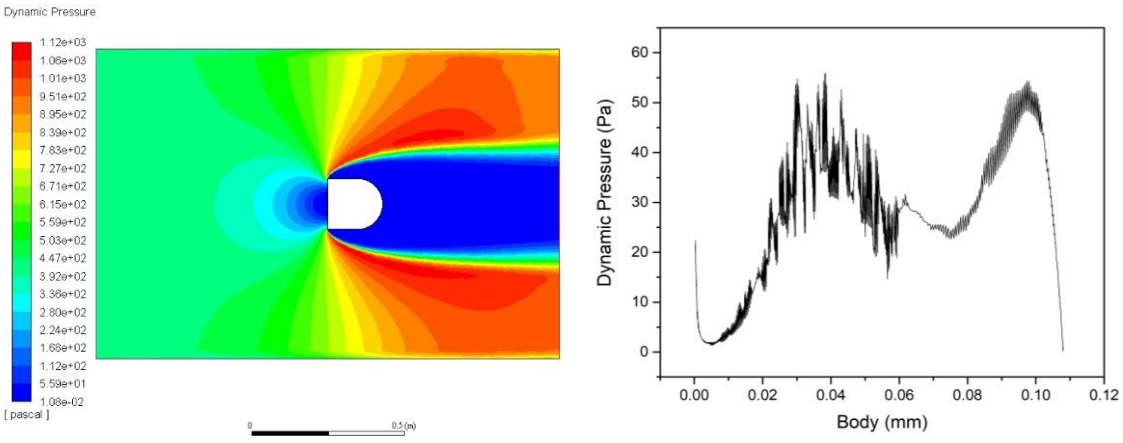

(a) (b)

Fig. 5. Dynamic Pressure (a) Contours (b) Plot

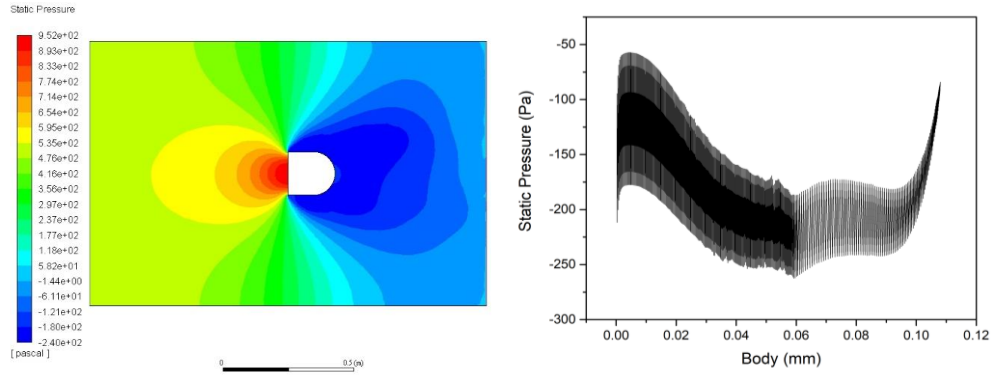

(a) (b)

Fig. 6. Static Pressure (a) Contours (b) Plot

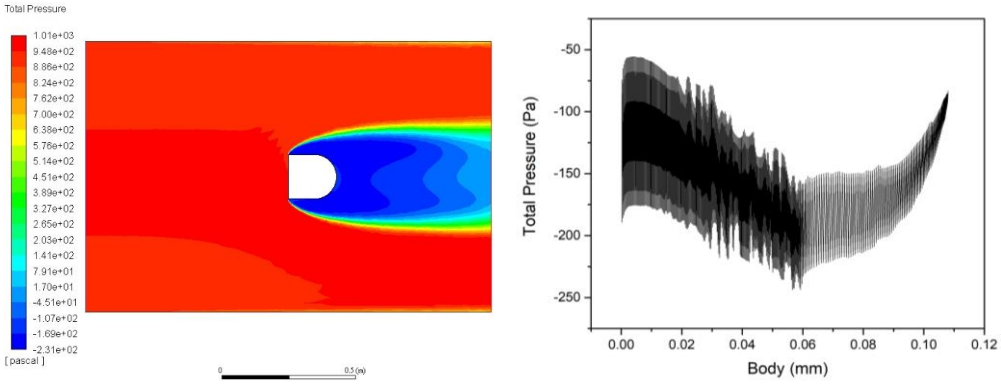

(a) (b)

Fig. 7. Total Pressure (a) Contours (b) Plot

3.1.2 Temperature distribution

This section shows the temperature variation from the inlet to the outlet of the 2D model of a bluff body without a square plate front body. This temperature variation consists of static temperature and total temperature. For the temperature variation, a numerical study was performed and results were validated for each case. Figure 8 and 9 show the static temperature and total temperature variation from the inlet to the outlet of the 2D model of a bluff body without a square plate front body by considering contours (Figure 8(a) and 9(a)) and plots respectively (Figure 8(b) and 9(b)).

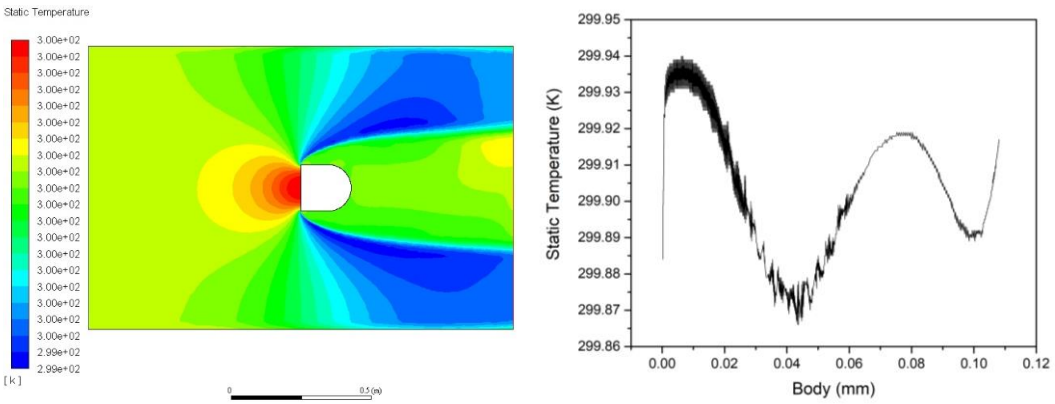

(a) (b)

Fig. 8. Static Temperature (a) Contours (b) Plot

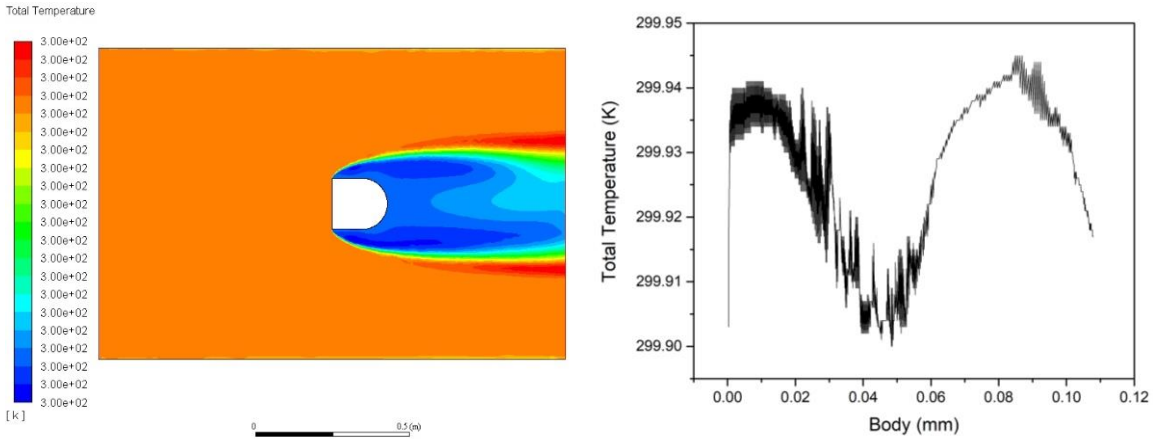

(a) (b)

Fig. 9. Total Temperature (a) Contours (b) Plot

3.1.3 Density distribution

In this section the density variation from the inlet to the outlet of the 2D model of a bluff body without a square plate front body. Figure 10 shows the density variation from the inlet to the outlet of the 2D model of a bluff body without a square plate front body by considering contours (Figure 10(a)) and plots (Figure 10(b)).

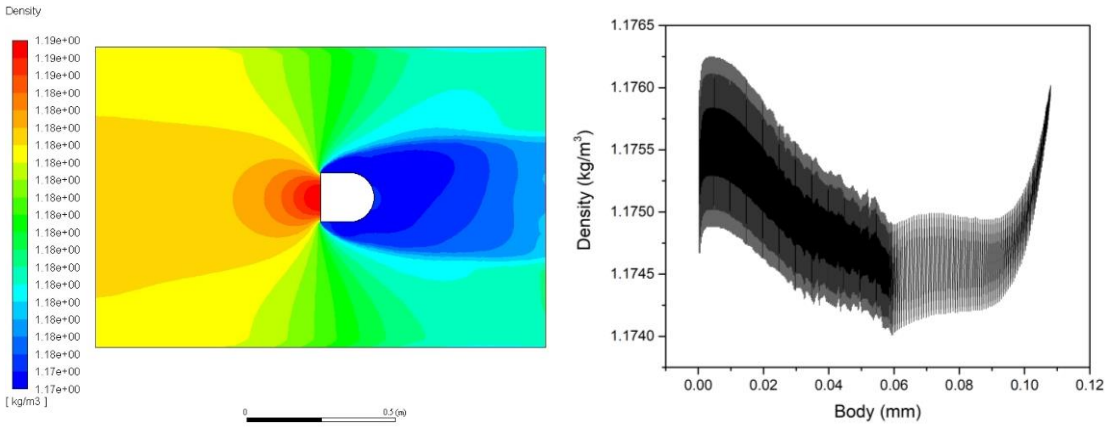

(a) (b)

Fig. 10. Density (a) Contours (b) Plot

3.1.4 Mach number

This part shows the velocity variation from the inlet to the outlet of the 2D model of a bluff body without a square plate front body. Figure 11 shows the Mach number variation from the inlet to the outlet of the 2D model of a bluff body without a square plate front body by considering contours (Figure 11(a)) and plots (Figure 11(b)).

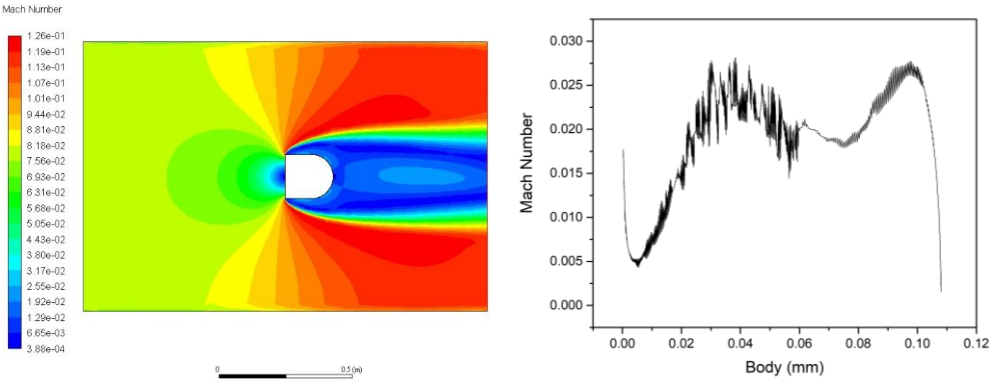

(a) (b)

Fig. 11. Mach Number (a) Contours (b) Plot

3.2 Without Pipe

3.2.1 Pressure distribution

In this section the pressure variation from the inlet to the outlet of the 2D model of a square plate front body of a bluff body. This pressure variation consists of dynamic pressure, static pressure, and total pressure. The Figure 12 to 14 show the dynamic pressure, static pressure and total pressure variation from the inlet to the outlet of the 2D model of a square plate front body of a bluff body by considering contours (Figure 12(a), 13(a) and 14(a)) and plots (Figure 12(b), 13(b) and 14(b)) respectively.

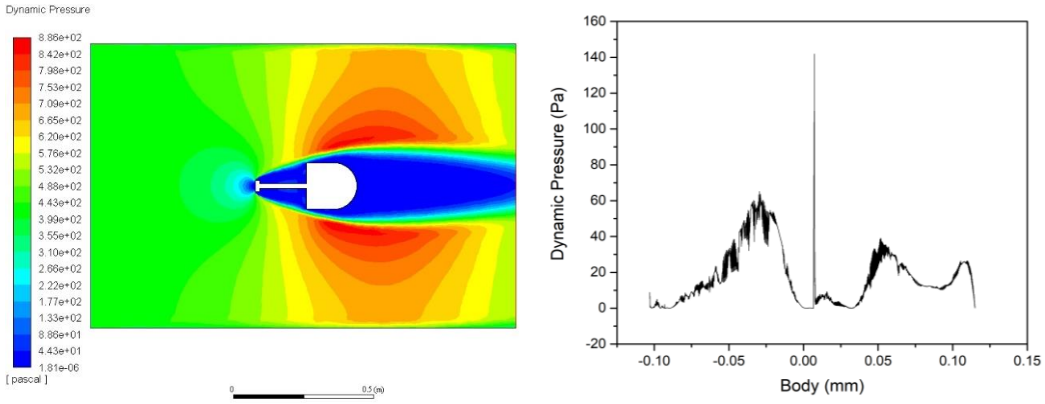

(a) (b)

Fig. 12. Dynamic Pressure (a) Contours (b) Plot

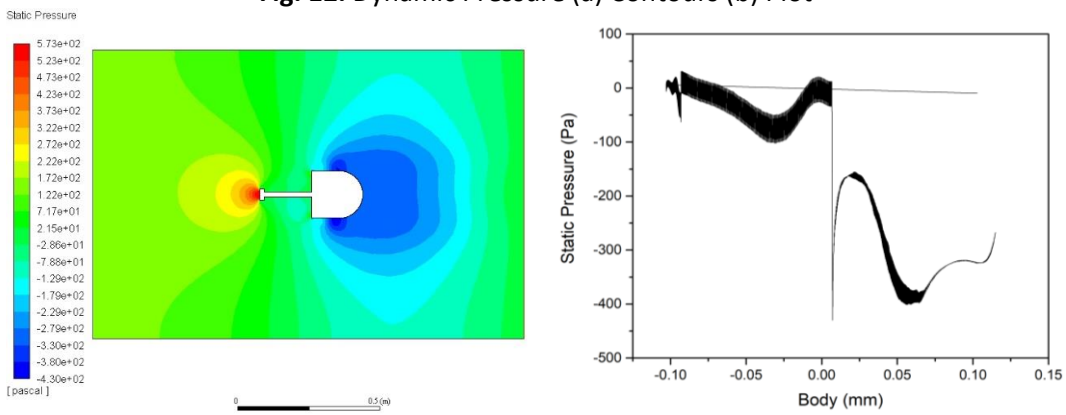

(a) (b)

Fig. 13. Static Pressure (a) Contours (b) Plot

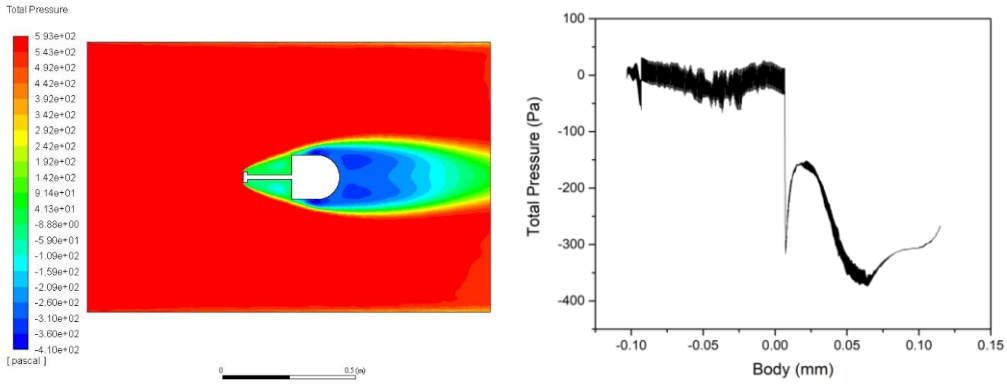

(a) (b)

Fig. 14. Total Pressure (a) Contours (b) Plot

3.2.2 Temperature distribution

The temperature variation from the inlet to the outlet of the 2D model of a square plate front body of a bluff body is shown in this section. This temperature variation consists of static temperature and total temperature. Figure 15 and 16 show the static temperature and total temperature variation from the inlet to the outlet of the 2D model of a square plate front body of a bluff body by considering contours (Figure 15(a) and 16(a)) and plots (Figure 15(b) and 16(b)) respectively.

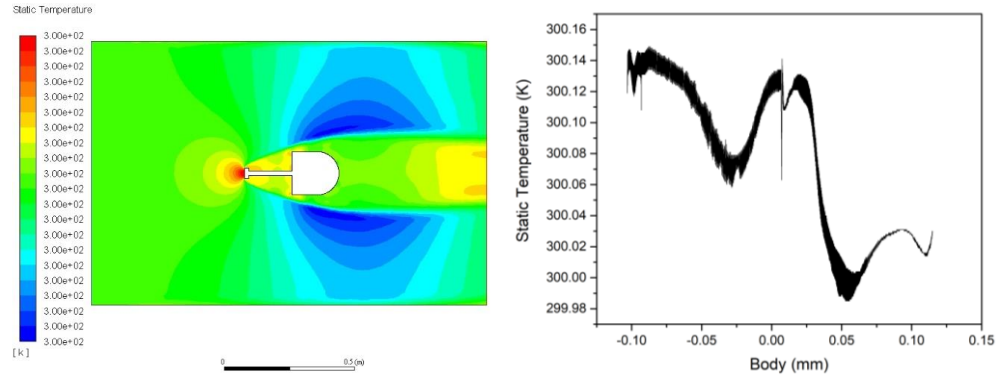

(a) (b)

Fig. 15. Static Temperature (a) Contours (b) Plot

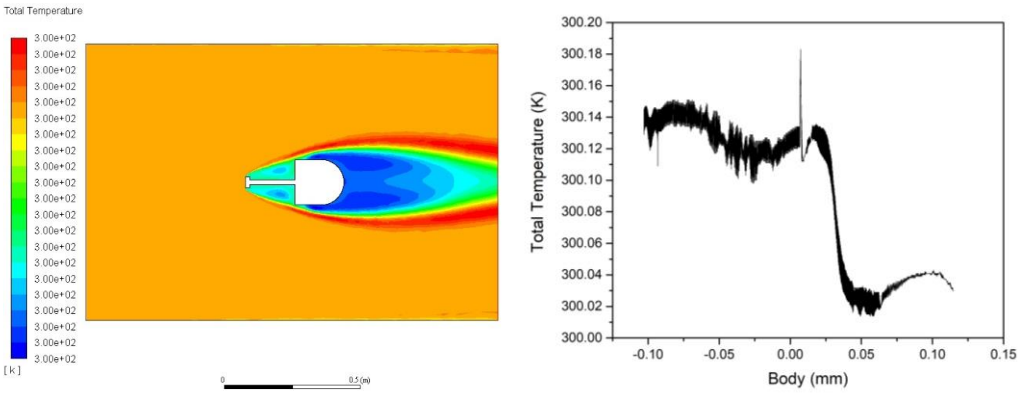

(a) (b)

Fig. 16. Total Temperature (a) Contours (b) Plot

3.2.3 Density distribution

In this section the density variation from the inlet to the outlet of the 2D model of a square plate front body of a bluff body. Figure 17 shows the density variation from the inlet to the outlet of the 2D model of a square plate front body of a bluff body by considering contours (Figure 17(a)) and plots (Figure 17(b)) respectively.

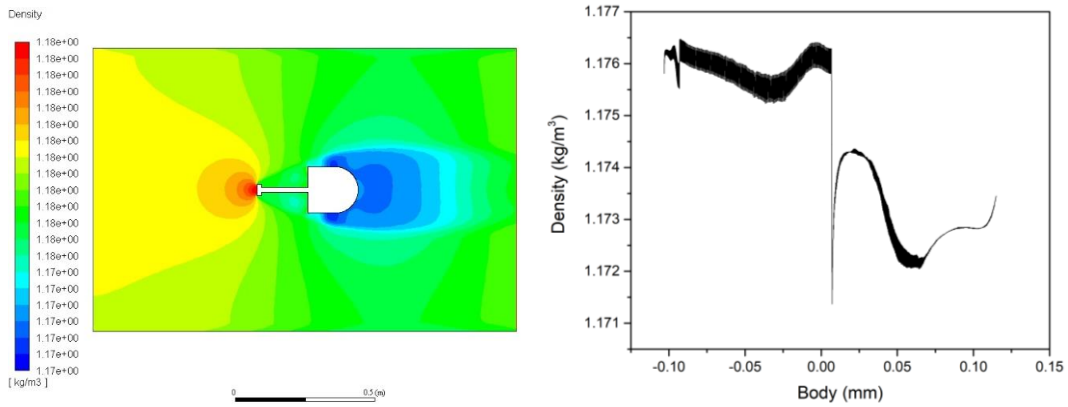

(a) (b)

Fig. 17. Density (a) Contours (b) Plot

3.2.4 Mach number

The velocity variation from the inlet to the outlet of the 2D model of a square plate front body of a bluff body is shown in this section. Figure 18 shows the Mach number variation from the inlet to the outlet of the 2D model of a square plate front body of a bluff body by considering contours (Figure 18(b)) and (Figure 18(b)).

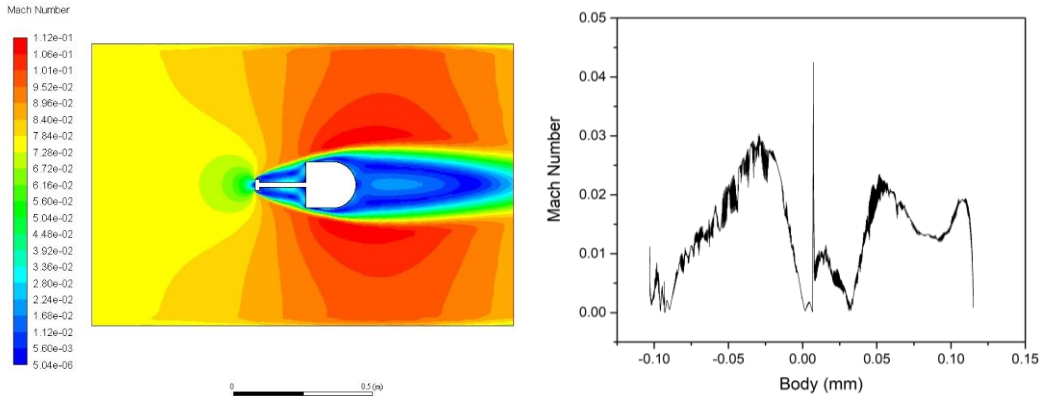

(a) (b)

Fig. 18. Mach number (a) Contours (b) Plot

4. Conclusions

The numerical investigation of the flow field of a non-circular cylinder has been successfully conducted by using an analytical and numerical method. The Bernoulli equation is used as was used by [1] for analytical calculation in ANSYS software. Furthermore, the ANSYS software is used to generate the non-circular cylinder flow field numerically and to prove the analytical method from the methods of papers [1,6]. From the simulation result, it can be seen a large wake zone at the back of

the non-circular cylinder. The streamlines of the flow field from the simulation result are smooth with the various colors are shown in the result. The difference between two cases which are without pipe and with a pipe, it shows the different flow field for both cases. The results show that the flow field from the numerical method is identical and being the same as the research papers from [1,6]. Where, the flow field can be seen very clearly.

Acknowledgment

This work was supported by the Research Fund FRGS 17-036-0602 provided by Malaysian Ministry of Education through International Islamic University Malaysia.

References

[1] Sowoud, Khalid M., and E. Rathakrishnan. "Front Body Effects on Drag and Flowfield of a Three-Dimensional Noncircular Cylinder" *AIAA journal* 31, no. 7 (1992): 401–403.
[2] M., Fharukh Ahmed G, Abdulrahman A. Alrobaian, Abdul Aabid, and S. A. Khan. "Numerical Analysis of Convergent-Divergent Nozzle Using Finite Element Method." *International Journal of Mechanical and Production Engineering Research and Development 8,* no. 6 (2018): 373–382.
[3] Khan, Sher Afghan, Abdul Aabid, and Maughal Ahmed Ali Baig. "CFD Analysis of CD Nozzle and Effect of Nozzle Pressure Ratio on Pressure and Velocity for Suddenly Expanded Flows." *International Journal of Mechanical and Production Engineering Research and Development (IJMPERD)* 8, no. 3 (2018): 1147–1158.
[4] Khan, Ambareen, Abdul Aabid, and Khan, Sher Afghan. "CFD Analysis of Convergent-Divergent Nozzle Flow and Base Pressure Control Using Micro-JETS." *International Journal of Engineering and Technology(UAE)* 7, no. 3.29 (2018): 232–235.
[5] Khan, Sher Afghan, Abdul Aabid, and C Ahamed Saleel. "CFD Simulation with Analytical and Theoretical Validation of Different Flow Parameters for the Wedge at Supersonic Mach Number." *International Journal of Mechanical and Mechatronics Engineering,* no. 1 (2019).
[6] Suresh, V., P. S. Premkumar, and C. Senthilkumar. "Drag Reduction of Non-Circular Cylinder at Subcritical Reynolds Numbers." *Journal of Applied Fluid Mechanics* 12, no. 1 (2019): 187–194.
[7] Libii, Josué Njock. "Using Wind Tunnel Tests to Study Pressure Distributions Around a Bluff Body: The Case of a Circular Cylinder." *World Transactions on Engineering and Technology Education* 8, no. 3 (2010): 361–366.
[8] Koenig, Keith, and Anatol Roshko. "An Experimental Study of Geometrical Effects on The Drag and Flow Field of Two Bluff Bodies Separated by a Gap." *Journal of Fluid Mechanics* 156 (1985): 167–204.
[9] Castro, I. P., and A. G. Robins. "The Flow Around a Surface-Mounted Cube in Uniform and Turbulent Streams" *Journal of fluid Mechanics* 90 (1977): 755–759.
[10] Gowda, B. H. L., H. J. Gerhardt, and C. Kramer. "Surface Flow Field Around Three-Dimensional Bluff Bodies" *Journal of Wind Engineering and Industrial Aerodynamics* 11 (1983): 405–420.
[11] Pamadi, B. N., C. Pereira, and B. H. Laxmana Gowda. "Drag Reduction by Strakes of Noncircular Cylinders" *AIAA journal* 26, no. 3 (1987): 292–299.
[12] Bearman, P. W. "Bluff body flows applicable to vehicle aerodynamics." *Journal of Fluids Engineering* 102, no. 3 (1980): 265-274.
[13] Tanner, M. "Reduction of Base Drag." *Progress in Aerospace Sciences* 16, no. 4 (1975): 369–384.
[14] Lomax, H, TH Pulliam, DW Zingg, and TA Kowalewski. "Fundamentals of Computational Fluid Dynamics." *Applied Mechanics Reviews* 55, no. 4 (2002): B61.
[15] Naga Sudhakar, B. V. V., B. Purna Chandra Sekhar, P Narendra Mohan, and Md Touseef Ahmad. "Modeling and Simulation of Convergent-Divergent Nozzle Using Computational Fluid Dynamics." *International Research Journal of Engineering and Technology (IRJET)* 3, no. 8 (2016): 346–350.
[16] Stefanou, George. "The Stochastic Finite Element Method: Past, Present, and Future." *Computer Methods in Applied Mechanics and Engineering* 198, no. 9–12 (2009): 1031–1051.
[17] Khan, Sher Afghan, Al Robian, Abdulrahman Abdulla, Asadullah, Mohammed, Khan, Abdul Mohsin. "Grooved Cavity as a Passive Controller behind Backward Facing Step." *Journal of Advanced Research in Fluid Mechanics and Thermal Sciences* 53, no. 2 (2019): 185–193.
[18] Khan, Sher Afghan, Al Robian, Abdulrahman Abdulla, and Mohammed Asadullah. "Threaded Spikes for Bluff Body Base Flow Control." *Journal of Advanced Research in Fluid Mechanics and Thermal Sciences* 53, no. 2 (2019): 194–203.
[19] Ilya Bashiera Hamizi, and Sher Afghan Khan."Aerodynamics Investigation of Delta Wing at Low Reynold's

Number." *CFD Letters* 11, no. 2 (2019): 32-41.
[20] Mohd Umair, Siddique, Sher Afghan Khan, Abdulrahman Alrobaian, and Emaad Ansari. "Numerical Study of Heat Transfer Augmentation Using Pulse Jet Impinging on Pin Fin Heat Sink," no. 576 (2018).
[21] Pathan, Khizar Ahmed, Sher Afghan Khan, and P. S. Dabeer. "CFD analysis of effect of area ratio on suddenly expanded flows." In *2017 2nd International Conference for Convergence in Technology (I2CT),* pp. 1192-1198. IEEE, 2017.
[22] Aabid, Abdul, Ambreen Khan, Nurul Musfirah Mazlan, Mohd Azmi Ismail, Mohammad Nishat Akhtar, and Sher Afghan Khan. "Numerical Simulation of Suddenly Expanded Flow at Mach 2.2." *International Journal of Engineering and Advanced Technology* 8, no. 3 (2019): 457–62.
[23] Khan, Sher Afghan, Abdul Aabid, and C Ahamed Saleel. "Influence of Micro Jets on the Flow Development in the Enlarged Duct at Supersonic Mach Number." *International Journal of Mechanical and Mechatronics Engineering* 19, no. 1 (2019): 70–82.
[24] Pathan, Khizar Ahmed, S. A. Khan, and P. S. Dabeer. "CFD analysis of effect of Mach number, area ratio and nozzle pressure ratio on velocity for suddenly expanded flows." In *2017 2nd International Conference for Convergence in Technology (I2CT),* pp. 1104-1110. IEEE, 2017.